Modifying Mg^{2+} Binding and Exchange with the N-Terminal of Calmodulin†

Svetlana B. Tikunova,*,‡ D. J. Black,‡ J. David Johnson,‡,± and Jonathan P. Davis§

Department of Molecular and Cellular Biochemistry, and Department of Physiology and Cell Biology, The Ohio State University, Columbus, Ohio 43210

Received September 11, 2000; Revised Manuscript Received January 10, 2001

ABSTRACT: To follow Mg^{2+} binding to the N-terminal of calmodulin (CaM), we substituted Phe in position 19, which immediately precedes the first Ca^{2+}/Mg^{2+} binding loop, with Trp, thus making F19WCaM (W−Z). W−Z has four acidic residues in chelating positions, two of which form a native Z-acid pair. We then generated seven additional N-terminal CaM mutants to examine the role of chelating acidic residues in Mg^{2+} binding and exchange with the first EF-hand of CaM. A CaM mutant with acidic residues in all of the chelating positions exhibited Mg^{2+} affinity similar to that of W−Z. Only CaM mutants that had a Z-acid pair were able to bind Mg^{2+} with physiologically relevant affinities. Removal of the Z-acid pair from the first EF-hand produced a dramatic 58-fold decrease in its Mg^{2+} affinity. Additionally, removal of the Z-acid pair led to a 1.8-fold increase in the rate of Mg^{2+} dissociation. Addition of an X- or Y-acid pair could not restore the high Mg^{2+} binding lost with removal of the Z-acid pair. Therefore, the Z-acid pair in the first EF-hand of CaM supports high Mg^{2+} binding primarily by increasing the rate of Mg^{2+} association.

Calmodulin (CaM)[1] is a ubiquitous Ca^{2+} binding protein that has two globular domains connected by a flexible central helix. Ca^{2+} binding to CaM causes the exposure of N- and C-terminal hydrophobic pockets, which allows CaM to bind and activate numerous target proteins (for review, see *1*). Each domain is capable of binding two Ca^{2+} ions through a pair of helix−loop−helix Ca^{2+} binding motifs, called EF-hands (numbered I−IV, starting at the N-terminal). The EF-hand Ca^{2+} binding motif was first deduced by Kretsinger and Nockolds (*2*) from the crystal structure of carp parvalbumin. Since then, this basic Ca^{2+} binding motif has been identified in numerous other proteins (for reviews, see *3*, *4*). Many theories exist on how EF-hands achieve their wide range of Ca^{2+} binding affinities and exchange rates (for review, see *5*).

Reid and Hodges (*6*) proposed the acid pair hypothesis, which correlates Ca^{2+} affinity with the number and position of acidic residues in chelating positions of the Ca^{2+} binding loop in an EF-hand. Ca^{2+} is ligated by seven oxygen atoms through six chelating residues in the loop, at positions 1(+X), 3(+Y), 5(+Z), 7(−Y), 9(−X), and 12(−Z), arranged on the axes of a pentagonal bipyramid (for reviews, see *7*, *8*). The hypothesis predicts that maximal Ca^{2+} affinity will be exhibited by an EF-hand that has four acidic residues in positions 1(+X), 5(+Z), 9(-X), and 12(−Z). Addition of a fifth acidic residue is supposed to reduce Ca^{2+} binding affinity, because of electrostatic repulsion. The acid pair hypothesis does not consider a Y-acid pair, because the residue in *−Y* position ligates Ca^{2+} through the peptide carbonyl oxygen and not through the carboxylate side chain. The acid pair hypothesis has been tested primarily using synthetic EF-hand peptides. Recently, the acid pair hypothesis received additional support, when Wu and Reid (*9*) and Wang et al. (*10*) measured the Ca^{2+} binding affinities of CaM mutants with mutated C-terminal residues in chelating positions.

Since Mg^{2+} is the most abundant divalent intracellular cation (for review, see *11*), it is not surprising that some Ca^{2+}binding EF-hands are also capable of binding Mg^{2+} with physiologically relevant affinities. Usually, the EF-hands that have high Ca^{2+} binding affinities also bind Mg^{2+}. For example, the third and fourth EF-hands of skeletal troponin C (sTnC), which bind Ca^{2+} with high affinity ($K_d = 50$ nM), also competitevely bind Mg^{2+} ($K_d = 0.2$ mM). The first and second EF-hands of TnC are considered to be Ca^{2+}-specific ($K_d = 3$ μM) (*12*). Because of the low resting Ca^{2+} concentration, Ca^{2+}/Mg^{2+} binding EF-hands are expected to be at least partially saturated with Mg^{2+}, since intracellular $[Mg^{2+}]_{free}$ is kept nearly constant in the low millimolar concentration range (*13*).

Unlike Ca^{2+}, which needs a 7-fold coordination, Mg^{2+} requires a 6-fold coordination (*14*). Mg^{2+}-bound EF-hand structures have been solved for pike parvalbumin (*15*), myosin regulatory light chain (*16*), and calbindin D_{9k} (*17*).

† This research was funded, in part, by NIH grant DK33727.

* To whom correspondence should be addressed: Department of Molecular and Cellular Biochemistry, The Ohio State University Medical Center, 333 Hamilton Hall, 1645 Neil Ave., Columbus, OH 43210-1218. Tel: 614-292-0104. Fax: 614-292-4118. E-mail: tikunova.1@osu.edu.

§ Department of Physiology and Cell Biology.

‡ Department of Molecular and Cellular Biochemistry.

± Deceased. Dedicated to the memory of J. David Johnson (03/11/1949−1/21/2000).

[1] Abbreviations: CaM, calmodulin; sTnC, skeletal troponin C.; Hepes, *N*-(2-hydroxyethyl)piperazine-*N*′-2-ethanesulfonic acid; MOPS, 3-(*N*-morpholino)propanesulfonic acid; EGTA, ethylene glycol bis(*β*-aminoethyl ether)-*N*,*N*,*N*′,*N*′-tetraacetic acid; EDTA, ethylenediamine-*N*,*N*,*N*′,*N*′-tetraacetic acid; W−Z, CaM mutant with the Phe 19 Trp mutation; F29WsTnC, sTnC mutant with Phe 29 Trp mutation; X, Y and Z, the acid pairs that are present in each Ca^{2+}binding loop; CaM-[loop 3X,Z], CaM with D95N, N79D, and S101D mutations in its third Ca^{2+} binding loop.

10.1021/bi0021333 CCC: $20.00
Published on Web 02/17/2001

In parvalbumin and myosin regulatory light chain, Mg^{2+} used the same ligands as Ca^{2+} with Glu in the −Z position acting as a monodentate ligand for Mg^{2+} but as a bidentate ligand for Ca^{2+}. In calbindin, a water molecule was inserted between Glu in the −Z position and Mg^{2+}. At the time of this publication, no Mg^{2+}-bound structure was available for CaM.

Mg^{2+} binding to CaM has been studied less extensively than Ca^{2+} binding. Unlike Ca^{2+}, Mg^{2+} binding to CaM does not lead to significant activation of CaM's target enzymes (*18*, *19*). However, since Mg^{2+} most likely competes for the same binding sites with Ca^{2+} (*18*−*20*), Mg^{2+} binding to CaM should affect CaM's response to changes in the intracellular Ca^{2+} concentration. In fact, Ohki et al. (*20*) observed that the affinity of Ca^{2+}-saturated CaM for some of its targets was decreased in the presence of excess Mg^{2+}. Therefore, detailed characterization of the Mg^{2+} binding properties of CaM is important. Recently, Ohki et al. (*20*) showed that Mg^{2+} first binds to the first and fourth EF-hands, and then to the second EF-hand. The third EF-hand exhibited the lowest Mg^{2+} affinity. The Mg^{2+} binding caused only local conformational changes within each of the Ca^{2+}/Mg^{2+} binding EF-hands, while Ca^{2+} binding led to global conformational changes in each domain. Malmendal et al. (*18*) recently determined Mg^{2+} affinities and dissociation rates for the first and second EF-hands of CaM using $^1H-^{15}N$ NMR. The second EF-hand showed a 2.2-fold lower Mg^{2+} affinity relative to the first EF-hand, which exhibited a 0.85 mM K_d for Mg^{2+}. The second EF-hand also exhibited an ∼26-fold faster Mg^{2+} dissociation rate than the first EF-hand.

Procyshyn and Reid (*21*) studied the effect of the number and location of acidic residues in chelating positions of the EF-hand on its Mg^{2+} binding affinity. They used 33-residue synthetic peptides to model the EF-hand and found that only peptides that had three or four acidic residues in chelating positions with a single acid pair on the Z-axis were able to bind Mg^{2+}. The Z acid pair was limited to Asp(+Z)-Glu(−Z) (*22*). In the present work, we wanted to see if these findings could be extended to an intact protein system.

To follow Mg^{2+} binding to the N-terminal of CaM, we substituted the Phe at position 19 with Trp, making F19WCaM (W−Z). We then introduced additional mutations (Figure 1), to determine the effect of acidic residues in chelating positions on the Mg^{2+} binding and exchange with the first EF-hand of CaM.

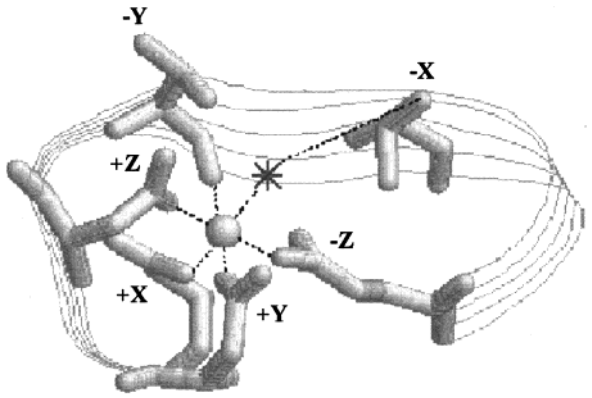

	20	22	24	26	28	31
	+X	+Y	+Z	-Y	-X	-Z
W-Z	D K D G D G T I T T K E					
W-0	D K D G N G T I T T K E					
W-X	D K D G N G T I D T K E					
W-Y	D K D G N G D I T T K E					
W-XY	D K D G N G D I D T K E					
W-XZ	D K D G D G T I D T K E					
W-YZ	D K D G D G D I T T K E					
W-XYZ	D K D G D G D I D T K E					

FIGURE 1: Theoretical model of Mg^{2+} coordination by the first EF-hand of CaM. The coordinates for the model were provided by Yves-Henry Sanejouand (*29*). The coordinates were obtained following the same protocol as for Figure 5 in (*29*). This figure was drawn using RasMol (*30*). The chelating oxygen atoms of the coordinating residues are shown to interact with the spherical Mg^{2+} ion by dashed lines. The water ligand is shown as an asterisk. Below are the amino acid sequences of the first Ca^{2+}/Mg^{2+} binding loop for CaM mutants. The amino acids in the loop are numbered 20−31, and the coordinating amino acids are labeled +X, +Y, +Z, −Y, −X, and −Z. Mutations are made at +Z, −Y, and −X positions, and the mutated residues are underlined.

EXPERIMENTAL PROCEDURES

Materials. Phenyl-Sepharose CL-4B, EDTA, and EGTA were purchased from Sigma Chemical Co. (St. Louis, MO). All other chemicals were of analytical grade.

Protein Mutagenesis and Purification. CaM mutants were constructed from a rat wild-type CaM plasmid by primer-selected site-directed mutagenesis using Stratagene's (La Jolla, CA) Quik-Change Site-Directed Mutagenesis Kit. The mutations were confirmed by DNA sequence analysis. The proteins were expressed in *Escherichia coli* and purified using Phenyl-Sepharose chromatography, as previously described (*23*). Protein concentrations were determined by an extinction coefficient of 7200 M^{-1} cm^{-1} at 280 nm.

Determination of Mg^{2+} Affinities. All static fluorescence measurements were performed using a Perkin-Elmer LS5 spectrofluorimeter at 22 °C. The free Mg^{2+} concentration was calculated using the webmax C program (http://www.stanford.edu/∼cpatton/maxc.html), as previously described (*24*). The Mg^{2+} affinity was reported as a dissociation constant (K_d). Each K_d represents an average of 3−5 titrations fit with the logistic sigmoid function, as previously described (*25*).

Determination of Mg^{2+} Dissociation Rates. The Mg^{2+} dissociation rate (K_{off}) was determined using an Applied Photophysics Ltd. (Leatherhead, UK) model SF.17 MV stopped-flow instrument, with a dead time of 1.6 ms at 10 °C. Each K_{off} represents an average of 10−15 traces, fit with a single exponential (variance $< 2 \times 10^{-4}$). The samples were excited using a 150 W xenon arc source. The emission was monitored through a UV-transmitting black-glass filter (UG1 from Oriel, Stanford, CT).

Determination of Mg^{2+} Association Rates. The Mg^{2+} association rate (K_{on}) was calculated using the relationship $K_{on} = K_{off}/K_d$, where K_{off} represents the release of a single Mg^{2+} ion and K_d represents the binding event of a single Mg^{2+} ion to the first EF-hand of CaM, assuming that W in position 19 only reports Mg^{2+} binding to the first EF-hand of CaM.

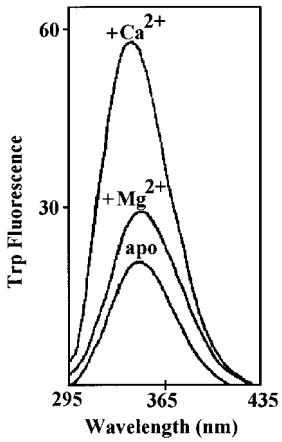

FIGURE 2: Effect of Ca^{2+} and Mg^{2+} on the fluorescence spectra of W−Z. Fluorescence emission spectra of W−Z in apo, + Mg^{2+}, or + Ca^{2+} states. The spectra were recorded with an excitation wavelength of 275 nm. W−Z concentration was 1 μM in 200 mM MOPS, 90 mM KCl, 2 mM EGTA, pH 7.0, at 22 °C. Trp fluorescence spectra were recorded before the addition of metals (apo), after the addition of either 40 mM Mg^{2+} (+ Mg^{2+}) or 1 mM Ca^{2+} (+ Ca^{2+}).

RESULTS

Effect of Ca^{2+}or Mg^{2+} on the Fluorescence Spectra of W−Z. To follow cation binding to the N-terminal of CaM, we substituted Phe 19, immediately preceding the first Ca^{2+}/Mg^{2+} binding loop, with Trp. Figure 2 shows fluorescence emission spectra of W−Z in the absence and in the presence of Ca^{2+} or Mg^{2+}. The W−Z protein underwent an ∼2.8-fold increase in its maximal Trp fluorescence intensity upon Ca^{2+} binding. Binding of Mg^{2+} to W−Z caused a smaller, ∼1.4-fold, increase in its maximal Trp fluorescence intensity. Binding of Ca^{2+} also induced a small blue shift in the maximal emission wavelength, from 345 to 340 nm, which was not observed upon Mg^{2+} binding. In fact, Mg^{2+} binding induced a small ∼2 nm red shift. These results suggest that the local environment of Trp 19 is more hydrophobic in the Ca^{2+} saturated state than in the Mg^{2+}saturated state.

Construction of Mutants and Their Mg^{2+} Binding Affinities. To determine the role of acid pairs in Mg^{2+} binding and exchange, we generated seven additional N-terminal CaM mutants. Addition of Ca^{2+} or Mg^{2+} led to changes in the fluorescence spectra of the mutants similar to that of W−Z (data not shown). Figure 3A shows the Mg^{2+}-dependent increase in Trp fluorescence that occurs when Mg^{2+} binds to the first EF-hand of W−Z, W−0, W−X, W−Y, and W−XY. W−Z exhibited a half-maximal Mg^{2+}-dependent increase in Trp fluorescence at 0.72 mM. Half-maximal Mg^{2+} binding for W−0, W−X, W−Y, and W−XY occurred at 42, 37, 10, and 11 mM, indicating 58-, 51-, 14-, and 15-fold decreases in Mg^{2+} affinity relative to that of W−Z, respectively. Figure 3B shows the Mg^{2+}-dependent increase in Trp fluorescence that occurs when Mg^{2+} binds to the first EF-hand of W−Z, W−XZ, W−YZ, and W−XYZ. Half-maximal Mg^{2+} binding occurred at 1.6, 0.40, and 0.74 mM for W−XZ, W−YZ, and W−XYZ, respectively. Therefore, W−XZ exhibited a 2.2-fold decrease in its Mg^{2+} affinity, relative to that of W−Z, while W−YZ showed a 1.8-fold increase in its Mg^{2+} affinity, relative to that of W−Z. The W−XYZ mutant's Mg^{2+} affinity was similar to that of W−Z.

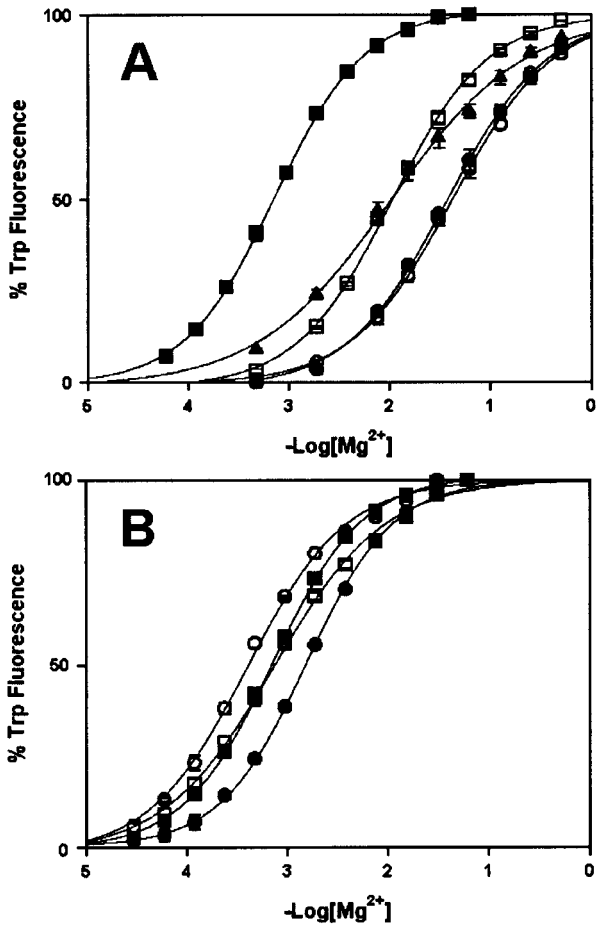

FIGURE 3: Mg^{2+} binding to the CaM mutants. (A) The Mg^{2+}-dependent increase in Trp fluorescence is shown as a function of $-Log[Mg^{2+}]$ for W−Z (■), W−0 (○), W−X(●), W−Y (▲), or W−XY (□). Increasing concentrations of Mg^{2+} were added to 1 mL of each protein (1 μM) in 200 mM MOPS, 90 mM KCl, 2 mM EGTA, pH 7.0, at 22 °C. One hundred percent fluorescence corresponds to a 1.4-, 1.3-, 1.3-, 1.4-, and 1.4-fold fluorescence increase for W−Z, W−0, W−X, W−Y, and W−XY, respectively. Trp fluorescence increase was monitored at 335 nm, with excitation at 275 nm. Each data point represents an average ± S.E. of 3−5 titrations. (B) The Mg^{2+}-dependent increase in Trp fluorescence is shown as a function of $-Log[Mg^{2+}]$ for W−Z (■), W−XZ (●), W−YZ (○), or W−XYZ (□). One hundred percent fluorescence corresponds to a 1.4-, 1.5-, 1.4, and 1.5-fold fluorescence increase for W−Z, W−XZ, W−YZ, and W−XYZ, respectively. The experimental conditions were the same as described for panel A.

The Hill coefficients for all eight mutants examined were close to unity, indicating the absence of Mg^{2+} binding cooprerativity between first and second EF-hands of CaM. One possible explanation is that Mg^{2+} binding to the second EF-hand does not lead to structural changes in the local environment of the first EF-hand.

Mg^{2+} Dissociation and Association Rates. We conducted fluorescence stopped-flow measurements, using EDTA-induced changes in Trp fluorescence, to determine the rates of Mg^{2+} dissociation from the first EF-hand of W−Z and the other CaM mutants. Figure 4A shows the rates of EDTA-induced decrease in Trp fluorescence for W−Z, W−0, W−X, W−Y, and W−XY. EDTA dissociated Mg^{2+} from the first EF-hand of W−Z, W−0, W−X, W−Y, and W−XY at rates of 139, 244, 222, 820, and 928 s^{-1}, respectively. Therefore, mutants W−0, W−X, W−Y, and W−XY exhibited 1.8-, 1.6-, 5.9-, and 6.7-fold faster Mg^{2+} dissociation

Table 1: Summary of Mg^{2+} Binding Properties for CaM Mutants[a]

nomenclature	mutant protein	acid pairs	K_d (mM)	Hill coeff	K_{off} (s^{-1})	K_{on} ($\times 10^5$ M^{-1} s^{-1})
W−Z	F19W	Z	0.72	1.0	139 ± 4	1.9
W−0	F19WD24N	none	42	0.9	244 ± 6	0.058
W−X	F19WD24NT28D	X	37	0.9	222 ± 22	0.06
W−Y	F19WD24NT26D	Y	10	0.7	820 ± 83	0.82
W−XY	F19WD24NT26DT28D	XY	11	0.9	928 ± 67	0.84
W−XZ	F19WT28D	XZ	1.6	1.0	257 ± 5	1.6
W−YZ	F19WT26D	YZ	0.40	0.9	323 ± 7	8.1
W−XYZ	F19WT26DT28D	XYZ	0.74	0.8	601 ± 45	8.1

[a] K_{on} values were calculated using the relationship $K_{on} = K_{off}/K_d$.

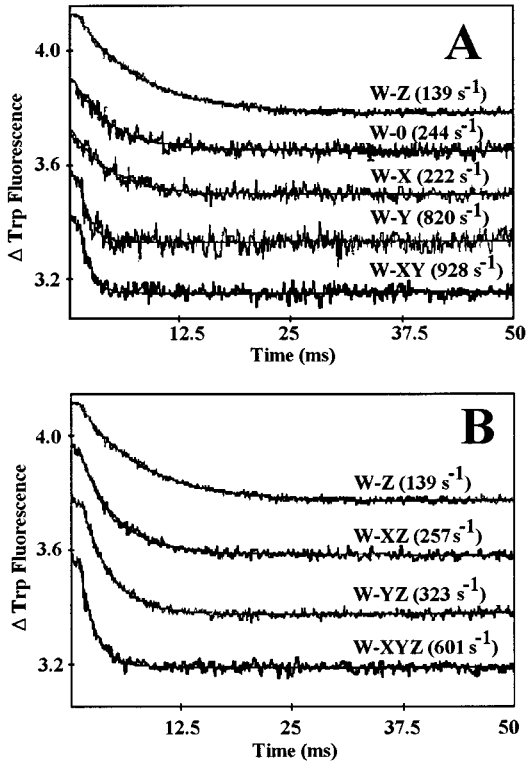

FIGURE 4: Rates of Mg^{2+} dissociation from the CaM mutants. (A) The time course of the decrease in Trp fluorescence is shown as EDTA dissociates Mg^{2+} from the N-terminal domain of W−Z, W−0, W−X, W−Y, or W−XY. Each protein (14 μM) in 200 mM HEPES, 500 μM EGTA, and 20 mM Mg^{2+} (pH 7.0) was rapidly mixed with an equal volume of 30 mM EDTA in 200 mM HEPES (pH 7.0), at 10 °C. Trp fluorescence was monitored through a UV-transmitting black glass filter (UG1 from Oriel, Stanford, CT) with excitation at 275 nm. The traces have been staggered for clarity. Each trace is an average of at least five traces, and the data were fit with a single exponential (variance < 2.0×10^{-4}). All kinetic traces were triggered at time zero, the first 1.6 ms of premixing is shown (the apparent lag phase), and the traces were fit after mixing was complete. Control experiments in which each protein (14 μM) in 200 mM HEPES, 500 μM EGTA, and 20 mM Mg^{2+} (pH 7.0) was mixed with an equal volume of 20 mM Mg^{2+} in 200 mM HEPES (pH 7.0) were flat lines. (B) The time course of the decrease in Trp fluorescence is shown as EDTA dissociates Mg^{2+} from the N-terminal domain of W−Z, W−XZ, W−YZ, or W−XYZ. The experimental conditions were the same as described for panel A.

rates, relative to that of W−Z. Figure 4B shows the rates of EDTA-induced decrease in Trp fluorescence for W−Z, W−XZ, W−YZ, and W−XYZ. Mg^{2+} dissociated from the first EF-hand of W−XZ, W−YZ, and W−XYZ at rates of 257, 323, and 601 s^{-1}, respectively. Therefore, mutants W−XZ, W−YZ, W−XYZ exhibited 1.8-, 2.3-, and 4.3-fold faster Mg^{2+} dissociation rates, relative to that of W−Z.

Having obtained the Mg^{2+} dissociation constants (K_d) and the Mg^{2+} dissociation rates (K_{off}), we calculated the Mg^{2+} association rates ($K_{on} = K_{off}/K_d$) for W−Z and its mutants. Table 1 compares the Mg^{2+} affinities (K_d), Hill coefficients, Mg^{2+} dissociation rates (K_{off}), and Mg^{2+} association rates (K_{on}) for W−Z and its mutants. Although the Mg^{2+} affinities of W−0 and W−X are 58- and 51-fold lower than that of W−Z, Mg^{2+} dissociation rates are only 1.8- and 1.6-fold faster, respectively. Therefore, the calculated Mg^{2+} on-rates for W−0 and W−X are 33- and 32-fold slower than that of W−Z, respectively. The mutant W−YZ, whose Mg^{2+} binding affinity was 1.8-fold higher than that of W−Z, showed a 2.3-fold faster Mg^{2+} dissociation rate, making its calculated Mg^{2+} on-rate ~4.3-fold faster than that of W−Z.

DISCUSSION

The goal of this study was to examine the effect of changing the number and location of acidic residues in chelating positions of the first EF-hand of CaM on the Mg^{2+} affinity of this EF-hand. The Ca^{2+}binding loop in the first EF-hand of CaM has Asp in positions 1(+X), 3(+Y), 5(+Z), and Glu in position 12(−Z). Therefore, it has four acidic residues in chelating positions, two of which are paired along the Z-axis. CaM has no intrinsic fluorescent probes on its N-terminal. To directly follow the Mg^{2+}-induced structural changes, we exchanged Trp for Phe in position 19, immediately preceding the first Ca^{2+}/Mg^{2+} binding loop. This mutation is analogous to the F29WsTnC mutation, which made possible determination of Ca^{2+} binding and exchange with the N-terminal sites of sTnC and its mutants (*26*). We then generated seven additional CaM mutants, in which the number of acid pairs was increased from zero to three, and examined their ability to bind Mg^{2+}. The Ca^{2+} and Mg^{2+} binding to all of these mutants resulted in Trp fluorescence increases, which allowed us to determine their Ca^{2+} and Mg^{2+} affinities. The Ca^{2+} results are discussed elsewhere (*25*). The increases in Trp fluorescence caused by Mg^{2+} were smaller than those caused by Ca^{2+}, which indicated that the local environment of Trp19 was different in the Mg^{2+} saturated state than in the Ca^{2+} saturated state. The W−Z protein exhibited half-maximal Mg^{2+} saturation at 0.72 mM, which is in excellent agreement with the K_d determined by NMR for the first EF-hand of CaM (*18*). We observed a dramatic 58-fold decrease in Mg^{2+} affinity of the first EF-hand when the native Z-acid pair was removed by replacing Asp in position +Z with Asn (mutant W−0). This same mutant exhibited only a 4-fold decrease in the N-terminal Ca^{2+} affinity (*25*). Therefore, in the first EF-hand of CaM, the presence of the native Z-acid pair was essential for high

Mg^{2+} binding. Consistent with our findings, Procyshyn and Reid (*21*) showed that only certain synthetic peptides that had a Z-acid pair were able to bind Mg^{2+}. Loop 3 of CaM has three acidic residues in positions +X, +Y, and −Z, but no acid pairs. Wang et al. (*10*) produced a CaM[loop 3X,Z] mutant that had four acidic residues, paired on the X- and Z-axes of the third loop. This CaM mutant exhibited only a 2.6-fold higher Mg^{2+} affinity as compared to that of the native CaM. However, the CaM[loop 3X,Z] mutant also had an additional mutation, replacing Asp in +Y position by Asn, which could explain why only a modest increase in affinity was observed. Consistent with our finding, Henzl et al. (*27*) increased the Mg^{2+} affinity of oncomodulin's CD-site ~50-fold by replacing the Ser residue in the +Z position with an Asp, therefore, producing a Z-acid pair and adding a fifth acidic chelating residue. Using $^1H-^{15}N$ NMR, Ohki et al. (*20*) determined that Mg^{2+} preferentially binds to the first and fourth EF-hands of CaM, which correlates with our data, since only the first and fourth EF-hands of CaM have endogenous Z-acid pairs.

The W−X mutant, which had four acidic residues in chelating positions, including an X-acid pair, exhibited only a 1.8-fold lower Ca^{2+} affinity relative to that of W−Z (*25*). This same mutant showed a dramatic 51-fold decrease in its Mg^{2+} affinity relative to that of W−Z. Therefore, an X-acid pair could not restore the high Mg^{2+} binding that was lost when the native Z-acid pair was removed. The addition of an X-acid pair on top of the Z-acid pair (W−XZ) caused a 2.2-fold decrease in Mg^{2+} affinity relative to that of W−Z, possibly because addition of a fifth acidic residue increased electrostatic repulsion. Wu and Reid (*9*) demonstrated that, when the fourth EF-hand was inactivated, the Ca^{2+} affinity of the third Ca^{2+} binding EF-hand of CaM was increased 58-fold upon introduction of an X-acid pair. Therefore, the X-acid pair plays a larger role in Ca^{2+} binding than it does in Mg^{2+} binding.

Interestingly, mutants W−Y and W−XY both showed ~4-fold increases in their Mg^{2+} affinities, relative to that of the W−0 protein. When the native Z-acid pair was present, the addition of a Y acid pair (W−YZ) caused a 1.8-fold increase in affinity relative to that of W−Z, despite the fact that the W−YZ mutant had five negatively charged residues in chelating positions. Therefore, Mg^{2+} binding was enhanced by replacing a Thr, in the −Y position, with a negatively charged Asp residue. Mutant W−XYZ exhibited a Mg^{2+} affinity similar to that of W−Z, indicating that the number of negatively charged residues is not as important as their location in determining Mg^{2+} binding affinity. In summary, the highest Mg^{2+} binding affinity to the first EF-hand of CaM was observed in the mutant W−YZ, which had both Y- and Z-acid pairs. The lowest Mg^{2+} binding affinity was observed in the mutant W−0, which had no acid pairs. Interestingly, for all of the mutants examined, the Hill coefficients were near unity, indicating the absence of Mg^{2+} binding cooperativity between the first and second EF-hands of CaM. Therefore, we propose that Mg^{2+} binding to the second EF-hand of CaM does not lead to changes in the local environment of Trp 19. This idea is consistent with the results of Ohki et al. (*20*), who showed that Mg^{2+} binding caused only local changes within each of the Ca^{2+}/Mg^{2+} binding loops, while Ca^{2+} binding led to global conformational changes in each domain.

We also studied Mg^{2+} dissociation from the first EF-hand of W−Z and mutants by monitoring rates of EDTA-induced decreases in Trp fluorescence. We observed Mg^{2+} dissociation from W−Z at 139 s^{-1} and 10 °C. After measuring the Q_{10} for W−Z at 1.8, we calculated the Mg^{2+} dissociation rate to be 375 s^{-1} at 25 °C. Using $^1H-^{15}N$ NMR, Malmendal et al. (*18*) determined that Mg^{2+} dissociated from the first EF-hand of CaM at 380 s^{-1} and 25 °C. Therefore, the Mg^{2+} dissociation rate obtained using our stopped-flow method was in excellent agreement with the Mg^{2+} dissociation rate measured by $^1H-^{15}N$ NMR. We also determined Mg^{2+} dissociation rates for the rest of the CaM mutants. Interestingly, mutant W−0, which exhibited a drastic 58-fold decrease in its Mg^{2+} affinity, showed only a 1.8-fold increase in its dissociation rate, relative to the W−Z protein. Thus, W−0 must have a 33-fold slower Mg^{2+} association rate, relative to the W−Z protein. Therefore, removal of the native Z-acid pair decreased Mg^{2+} affinity by both a large decrease in the Mg^{2+} association rate coupled with a small increase in the Mg^{2+} dissociation rate.

According to the gateway hypothesis, an EF-hand that has a negatively charged residue in the −X position should have a slower cation dissociation rate than an EF-hand that has a neutral residue in that position (*28*). Contrary to the gateway hypothesis, mutant W−X (gateway residue Asp) showed a Mg^{2+} dissociation rate similar to that of W−0 mutant (gateway residue Thr). Mutant W−XZ (gateway residue Asp) exhibited a 1.8-fold faster Mg^{2+} dissociation rate than W−Z protein (gateway residue Thr). Mutant W−XYZ (gateway residue Asp) displayed a 1.9-fold faster Mg^{2+} dissociation rate than mutant W−YZ (gateway residue Thr). Clearly, other factors govern Mg^{2+} dissociation rates from the first N-terminal EF-hand of CaM. Consistent with our findings, Malmendal et al. (*18*) observed that Mg^{2+} dissociated from the second EF-hand of CaM (gateway residue Asp) ~26-fold faster than it did from the first EF-hand (gateway residue Thr).

Mutant W−Y exhibited a 3.4-fold faster Mg^{2+} dissociation rate than mutant W−0. Mutant W−YZ exhibited a 2.3-fold faster Mg^{2+} dissociation rate than mutant W−Z. Therefore, an Asp in the −Y position increases Mg^{2+} dissociation rates, Mg^{2+} binding affinities, and Mg^{2+} association rates. It is possible that a negatively charged residue in the −Y position increases Mg^{2+} binding affinity by forming favorable ionic interactions with the solvent or other residues to stabilize the Mg^{2+} bound state of the mutant CaM.

In conclusion, we have shown that an endogenous Z-acid pair in the first EF-hand of CaM was required for high Mg^{2+} affinity. Removal of the Z-acid pair had a much more dramatic effect on the Mg^{2+} affinity (~58-fold decrease) than on Ca^{2+} affinity (~4-fold decrease). Addition of X- or Y-acid pairs could not restore high Mg^{2+} binding lost with removal of the endogenous Z-acid pair. We have also demonstrated that a Z-acid pair was able to support high Mg^{2+} affinity of the first Ca^{2+}/Mg^{2+} binding EF-hand of CaM primarily by increasing the Mg^{2+} association rate.

ACKNOWLEDGMENT

We appreciate the critical reading of the manuscript by Dr. Ruth A. Altschuld, Dr. Jack A. Rall, Dr. Russ Hille, and Dr. Anthony R. Means.

REFERENCES

1. Van Eldik, L. J., and Watterson, D. M., Eds. (1998) in *Calmodulin and Signal Transduction*, Academic Press, New York.
2. Kretsinger, R. H., and Nockolds, C. E. (1973) *J. Biol. Chem. 248*, 3313−3326.
3. Nelson, M. R., and Chazin, W. J. (1998) *Biometals 11*, 297−318.
4. Ikura, M. (1996) *Trends Biochem. Sci. 21*, 14−17.
5. Falke, J. J., Drake, S. K., Hazard, A. L., and Peersen, O. B. (1994) *Q. Rev. Biophys. 27*, 219−290.
6. Reid, R. E., and Hodges, R. S. (1980) *J. Theor. Biol. 84*, 401−444.
7. Kawasaki, H., Nakayama, S., and Kretsinger, R. H. (1998) *Biometals 11*, 277−295.
8. Yap, K. L., Ames, J. B., Swindells, M. B., and Ikura, M. (1999) *Proteins 37*, 499−507.
9. Wu, X., and Reid, R. E. (1997) *Biochemistry 36*, 8649−8656.
10. Wang, S., George, S. E., Davis, J. P., and Johnson, J. D. (1998) *Biochemistry 37*, 14539−14544.
11. Birch, N. J., Ed. (1993) in *Magnesium and the Cell*, Academic Press Ltd., London.
12. Potter, J. D., and Gergely, J. (1975) *J. Biol. Chem. 250*, 4628−4633.
13. Williams, R. J. P. (1993) in *Magnesium and the Cell* (Birch, N. J., Ed.) pp 15−30, Academic Press Ltd., London.
14. Martin, R. B. (1984) in *Metal Ions in Biological Systems* (Sigel, H., Ed.) pp 1−49, Academic Press, New York.
15. Declercq, J. P., Tinant, B., Parello, J., and Rambaud, J. (1991) *J. Mol. Biol. 220*, 1017−1039.
16. Houdusse, A., and Cohen, C. (1996) *Structue 4*, 21−32.
17. Andersson, M., Malmendal, A., Linse, S., Ivarsson, I., Forsen, S., and Svensson, L. A. (1997) *Protein Sci. 6*, 1139−1147.
18. Malmendal, A., Evenas, J., Thulin, E., Gippert, G. P., Drakenberg, T., and Forsen, S. (1998) *J. Biol. Chem. 273*, 28994−29001.
19. Malmendal, A., Linse, S., Evenas, J., Forsen, S., and Drakenberg, T. (1999) *Biochemistry 38*, 11844−11850.
20. Ohki, S., Ikura, M., and Zhang, M. (1997) *Biochemistry 36*, 4309−4316.
21. Procyshyn, R. M., and Reid, R. E. (1994) *J. Biol. Chem. 269*, 1641−1647.
22. Reid, R. E., and Procyshyn, R. M. (1995) *Arch. Biochem. Biophys. 323*, 115−119.
23. George, S. E., Su, Z., Fan, D., and Means, A. R. (1993) *J. Biol. Chem. 268*, 25213-2520.
24. Bers, D. M., Patton, C. W., and Nuccitelli, R. (1994) in *Methods in Cell Biology* (Nuccitelli, R., Ed.) pp 3−29, Academic Press, San Diego.
25. Black, D. J., Tikunova, S. B., Johnson, J. D., and Davis, J. P. (2000) *Biochemistry 39*, 13831−13837.
26. Johnson, J. D., Nakkula, R. J., Vasulka, C., and Smillie, L. B. (1994) *J. Biol. Chem. 269*, 8919−8923.
27. Henzl, M. T., Hapak, R. C., and Goodpasture, E. A. (1996) *Biochemistry 35*, 5856−69.
28. Renner, M., Danielson, M. A., and Falke, J. J. (1993) *Proc. Natl. Acad. Sci. 90*, 6493−6497.
29. Allouche, D., Parello, J., and Sanejouand, Y.-H. (1999) *J. Mol. Biol. 285*, 857−873.
30. Sayle, R. A., and Milner-White, E. J. (1995) *Trends Biochem. Sci. 20*, 374−376.

BI0021333